Measurements of Magnetic Permeability and H_c of Magnet Steels using Digital Techniques*

R. Thomas and G. Morgan
Accelerator Development Department
Brookhaven National Laboratory
Upton, New York 11973-5000

Abstract

The magnet-to-magnet variations in the dipole field of superconducting accelerator magnets must fall within specified tolerances to avoid excessive beam losses during injection. At injection field levels (~0.4 T for RHIC), the variations in the field attributable to the iron arise from variations in the chemical impurities, cold working and heat treatment. These structure-sensitive effects can be characterized by measuring the permeability and coercive force, H_c, of iron samples.

A digital permeameter was developed to perform precise measurements of the magnetic properties of ring samples. An arbitrary function generator and two high-precision digital multimeters were connected to a desktop computer using the IEEE-488 bus, and software was written to automatically acquire and analyze the data. Through the use of the arbitrary waveform generator, the effect of varying the period of the *B-H* loop and the effect of varying the shape of the *H* waveform were explored.

The effects of annealing, bending and flattening, and temperature on H_c and the relative permeability have been investigated for samples of magnet steel from several manufacturers.

I. Sample Description

The ring samples were cut from 0.250 plate and have an inner diameter of 2.00 and an outer diameter of 2.3750. Two, multi-layer, toroidal coils are wound on each sample—an inner pickup coil, designated the *B* coil, and an outer coil for applying the magnetizing force, the *H* coil. The measurements on twenty-two ring samples of magnet steel are reported here. The first ten ring samples were initially wound and measured by an outside vendor. These samples have 300 turns in the *H* coil and 100 turns in the *B* coil. The other twelve ring samples have an *H* coil of 632 turns and a *B* coil of 1000 turns in order to improve the resolution of the measurements. In addition, a brass ring sample was prepared in the same manner as the latter twelve steel samples to allow the determination of the small correction that must be made for the air flux in the *B* coil.

Table I describes the ring samples.

II. Measurement Set-up

The measurements that had been performed by the outside vendor used a dc electronic hysteresigraph in accordance with ASTM test method A-773 in which the values of interest are read from a plot of the dc magnetization curve. These results, however, had neither the resolution nor the reproducibility required. As precision measuring instruments were already available in the Magnet Division, a decision was made to use these devices in conjunction with a desktop workstation to form a digital permeameter.

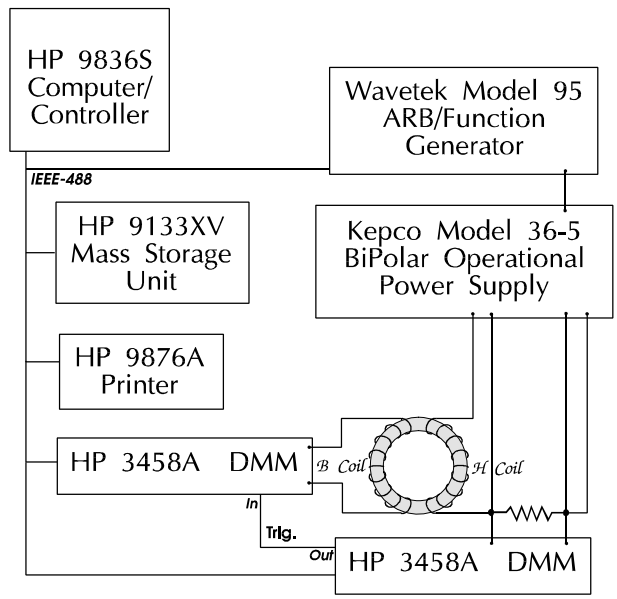

Figure 1. Experimental set-up for ring sample measurements.

As seen in Figure 1, the current in the *H* coil is derived from a bipolar operational power supply. A digital multimeter samples and stores the value of the voltage drop across a resistor in series with the coil. A second digital multimeter, which is triggered by the first, measures and stores the value of the voltage induced in the *B* coil as a result of the changing flux.

The output of the bipolar operational power supply is controlled by the computer indirectly through commands to a function generator. Once the waveforms have been acquired by the multimeters, the data are retrieved by the computer, analyzed, plotted, and stored.

III. Data Reduction

The magnetizing force, *H*, for the *k*th reading is given by

$$H_k(\mathrm{Oe}) = \frac{4\pi}{10}\,\frac{N_H\, I_{H,k}}{l}$$

where $I_{H,k}$ is calculated using the voltage value, $V_{H,k}$ stored by the multimeter connected to the resistor in series with *H* coil, and *l* is the mean magnetic length, which, in the case of ring samples, is the mean circumference. The flux change ΔN_k that corresponds to the calculated H_k is given by

*Work supported by the U. S. Department of Energy.

Table I. Magnet-Steel Ring Samples

Sample No.	Source	Comments	Location
1	LTV	Non-annealed	Beginning of coil (LNA)
2	LTV	Non-annealed	Middle of coil (LNA)
3	LTV	Non-annealed	End of coil (LNA)
4	LTV	Fully annealed	Beginning of coil (LFA)
5	LTV	Fully annealed	Middle of coil (LFA)
6	LTV	Fully annealed	End of coil (LFA)
7	Inland	50490	
8	LTV	Non-annealed—then annealed finished ring at 750E C for 2 hrs.	(LNA)
9	LTV	Fully annealed—then annealed finished ring at 750E C for 2 hrs.	(LFA)
10	Inland	50490—Annealed finished ring at 750E C for 2 hrs.	
11	Nippon	Non-annealed	RHIC lamination (same lamination)
12	Nippon	Non-annealed	
13	Nippon	Fully annealed	SSC lamination (same lamination)
14	Nippon	Fully annealed	
16	Inland	50490	same lamination
17	Inland	50490	
18, 19, 20	Inland	50490	Before coiling.
21, 22, 23	Inland	50490	After coiling on a coil i.d. of 240 and subsequent straightening.

$$)\,N_k \text{ (maxwells) } ' \;\&\; \frac{10^8}{N_B}\; V_{B,k}\;)\,t$$

The flux density change, $)\,B$ (gauss), is computed using the cross-sectional area of the specimen and the appropriate area correction factor.

The measurement of V_H is straightforward. The voltage on the B coil, however, is often small. If the range of the H sweep is large, V_B will be large during only two short periods of the cycle that are relatively near the time where $H(t)$ crosses zero, as shown in Figure 2. On the other hand, digital multimeters have a speed versus resolution trade-off. Each reading of the multimeter is actually a sample of the voltage signal over

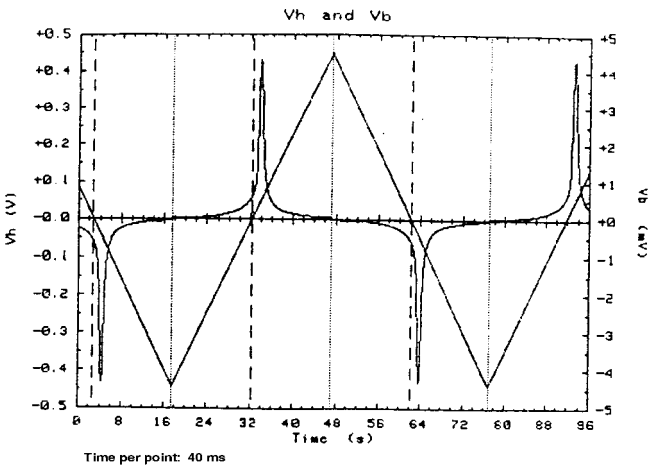

Figure 2. Linear ramp, V_h, and B coil signal, V_b.

a programmable time interval (the aperture or integration time of the multimeter's analog-to-digital convertor). For the ring samples being measured, noise rejection and resolution were more important, so the multimeters were programmed to use one or more power line cycles for each reading; thus providing 25 bits of resolution (7.5 digits) and >60 dB normal mode rejection at 60 Hz. For low field measurements, $H_{max} < 10$ Oe, the function generator was programmed to produce a simple triangular waveform, but for larger sweeps, the waveform was changed to one that moved slowly through the region near zero and much more rapidly at the extremes. This was achieved by calculating a waveform based on the tangent function and loading it into the function generator. A waveform that goes as $\tan(t)$ not only increases the signal voltage in the region where μ is low, it also minimizes the heating in the windings of the H coil. (See Figure 3.)

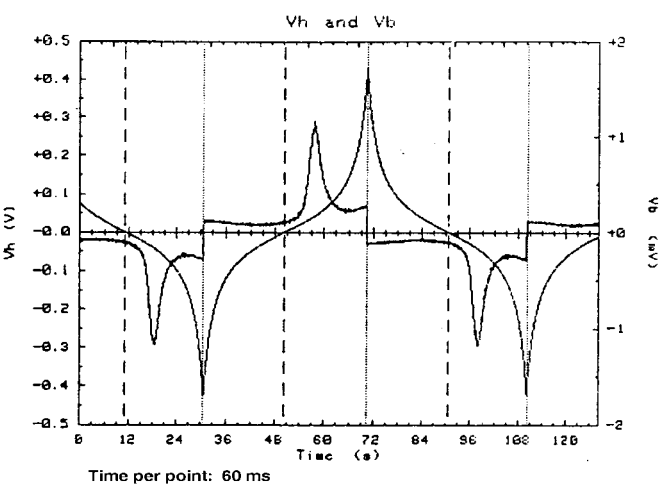

Figure 3. Non-linear V_h ramp and resulting signal, V_b.

The software determines the zero-crossings of the V_H and V_B signals. The zero-crossing is found by searching for a sign change in the values, fitting a straight line to the five points on either side of the point where the sign changed, and interpolating. Thus, the zero-crossings do not, in general, correspond to a measured point. Corrections are applied in subsequent calculations to take this fact into account. If the sum of the V_B values between the first and third zero-crossings is not zero, then a "drift correction" offset is applied. (This will force the hysteresis loop to close.) It then computes the sum of the) Bs from the first to the third zero-crossings of V_B, and also the sum of *) B* over the same region. B_{max} is then assumed to be one-fourth the sum of the absolute values of the) Bs, and the computed B values are appropriately offset and plotted against H to produce the hysteresis loop as shown in Figure 4.

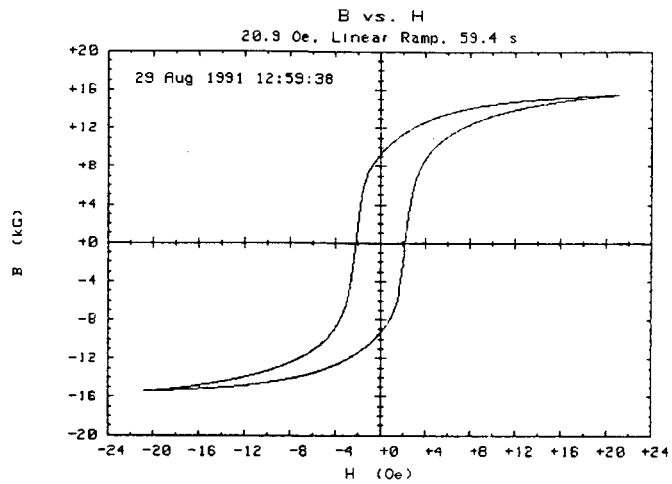

Figure 4. Hysteresis loop for a magnet steel ring sample.

The measurements performed on each sample are given in Table II.

Table II. Measurements performed on each ring sample.

***H_c* Measurements**
Ramp Amplitudes: ±10, ±30, ±100 Oe Loop Periods: 10 s, 15 s, 20 s, 25 s, 30 s, 40 s, 50 s, 60 s, 70 s, 85 s, 100 s (33 H_c measurements per sample)
Relative Permeability Measurements
Determined from loop tips at 23 ramp amplitudes: 0.4, 0.5, 0.6, 0.8, 1.0, 1.4, 1.8, 2.2, 2.6, 3.0, 3.4, 4.0, 5.0, 6.0, 8.0, 10, 15, 20, 30, 40, 60, 80, 100 Oe All loop periods, 30 s. Ramp amplitudes of less than ±10 Oe were linear ramps.

Typical results are shown in Figures 5.

IV. Results and Discussion

The Relativistic Heavy Ion Collider (RHIC) is a synchrotron particle accelerator composed of two rings. Its design allows heavy nuclei to be collided at ultra-relativistic energies. The two beams of heavy ions are constrained to follow a closed

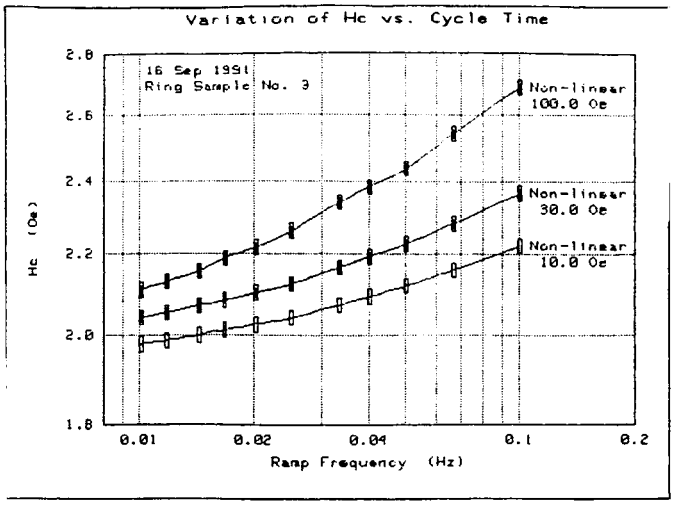

Figure 5. H_c as a function of the sweep rate for three values of H_{max}.

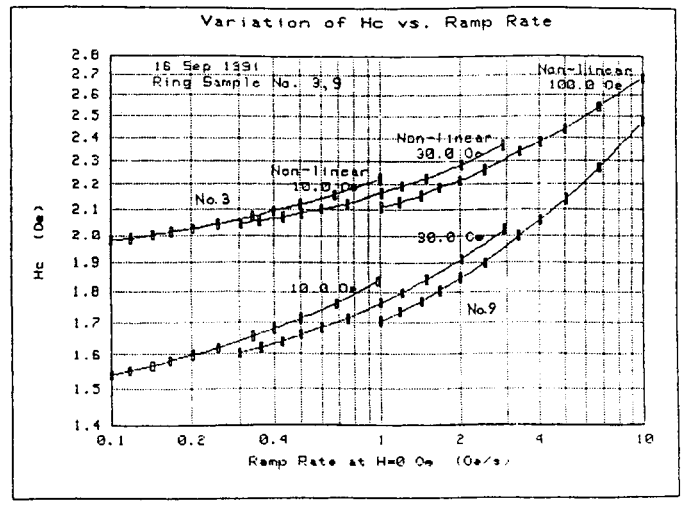

Figure 6. Variation of H_c with sweep rate.

orbit by 372 superconducting dipole magnets. At injection (0.4 T), field distortion due to superconductor magnetization is large, and it is necessary to ensure that field errors that are caused by variations in the magnet steel do not exacerbate the problem. The tolerance on the variation of the dipole field from magnet to magnet is ~2 gauss r.m.s. [1] The ramp rate in the RHIC dipoles is low, so hysteresis loss is not itself an important consideration. However, the coercivity H_c and the permeability at low-field (μ at H = 1 Oe) are known to be correlated [2]. It is often easier to obtain a high resolution measurement of H_c than it is to measure μ(H= 1 Oe) precisely.

Unlike the SSC magnets, RHIC magnet steel must have a high yield strength. The structural changes required to achieve this higher yield strength (e.g., cold working or the introduction of impurities) will also affect the permeability and coercivity [3].

At 10 Oe, the limits on the variation of the average permeability from magnet to magnet are not as stringent as at low fields. The field tolerances can be met if μ always falls in the range 1290 – 1650. Only three of the measured ring samples had μ values at H = 10 Oe that fell outside this range.

At 100 Oe, the value of the permeability becomes more sensitive to chemistry than to structure. For RHIC, the permeability at 100 Oe is expected to fall in the range 181 to 188 if the low field specifications are satisfied.

H_c Results

The value of H_c is clearly dependent upon the sweep rate, and asymptotically approaches a lower limit as the rate decreases. The limit is, as expected, lower for annealed samples than for non-annealed samples. Also, the H_c of the annealed samples varies more rapidly with ramp rate than does the H_c of the non-annealed samples, as shown in Figure 6. As the data were taken with a non-linear sweep rate, the H_c values are plotted against the sweep rate at H = 0.

The H_c values obtained for all the samples, for H_{max}=100 Oe and a sweep rate of 100 s for the full loop, are given in Table III.

It is noted that the H_c values for annealed ring samples from one manufacturer (Ring Nos. 8 and 9) were higher (1.67 versus 1.01) than the values for fully annealed samples from another (Ring Nos. 13 and 14). Since the differences in the chemistry of these samples are small, the difference must be due to other structural effects, perhaps the crystal size.

Table III. H_c at 100 Oe, 100 s.

Sample No.	H_c (Oe)	Sample No.	H_c (Oe)
1	2.10	12	1.81
2	2.05	13	0.959
3	2.11	14	1.06
4	2.05	16	2.08
5	2.10	17	2.09
6	2.05	18	2.18
7	2.04	19	2.03
8	1.65	20	2.06
9	1.70	21	2.39
10	1.65	22	2.36
11	1.52	23	2.36

Effect of Temperature

Ring Sample No. 7, which was not annealed after having been machined, was also measured while immersed in liquid nitrogen. For 100 s loop periods, the H_c increased when the temperature was lowered as shown in Table IV.

Table IV. Variation of H_c with Temperature and Field Amplitude

H_{max} 6	10 Oe	30 Oe	100 Oe
room temperature	1.92	1.98	2.03
liquid nitrogen temperature	2.31	2.45	2.67

Although the low temperature permeability exceeded the room temperature permeability at high fields, it was less than the room temperature permeability for fields less than 15 Oe. Also, the peak in the relative permeability moved from 3 Oe to 3.7 Oe when the temperature was lowered. (See Figure 7.)

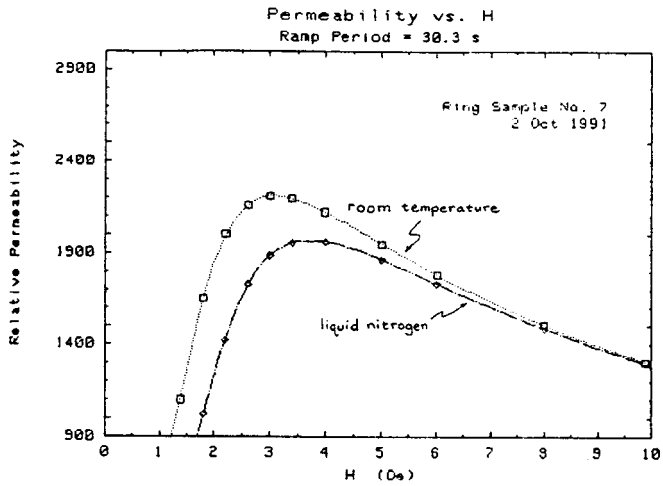

Figure 7. Relative permeability at two temperatures.

Effect of Coiling

Two pieces were cut from a single flat plate of 0.250 steel. One piece was bent around a cylindrical form having a diameter of 240 and then reflattened. Three rings were machined from each piece. One of the three unbent ring samples, Ring Sample No. 18, gave anomalous results; perhaps as a result of inhomogeneity in the sample or to improper machining of the ring. The H_c values for Ring Sample No. 20 (unbent) and Ring Sample No. 23 (bent and reflattened) are compared in Figure 8.

Ring Sample Nos. 19 and 20 (unbent) had $H_c = 2.046 \pm 0.02$, while H_c for the three bent and reflattened rings (Nos. 21, 22 and 23) was 2.37 ± 0.02. So although the value increased, probably because the bending introduced additional structure, the spread in the measured value of H_c did not change—at least for this small sample. On the other hand, it is plausible to assume that the increase is in proportion to the bend curvature, so that material with less curvature from the outer part of a coil would have less increase in H_c, causing an increase in the spread.

The relative permeability of these rings also differed markedly; it was reduced in the bent and reflattened samples. The peak permeability decreased from ~2700 to ~1900. The results are shown in Figure 9.

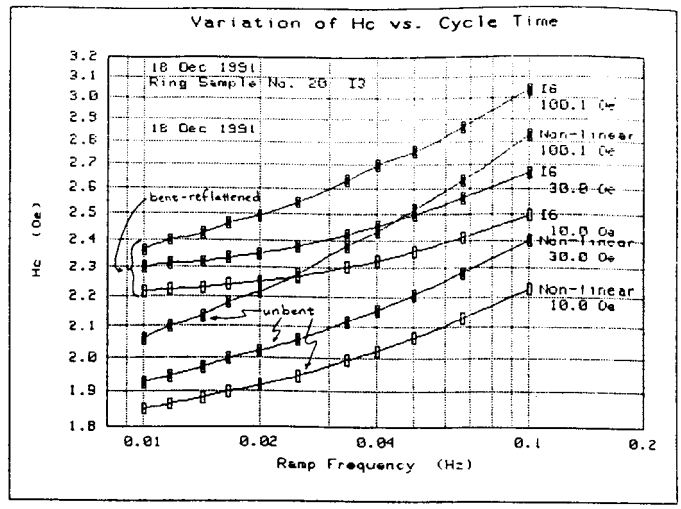

Figure 8. H_c results for bent (I6) and unbent (I3) ring samples.

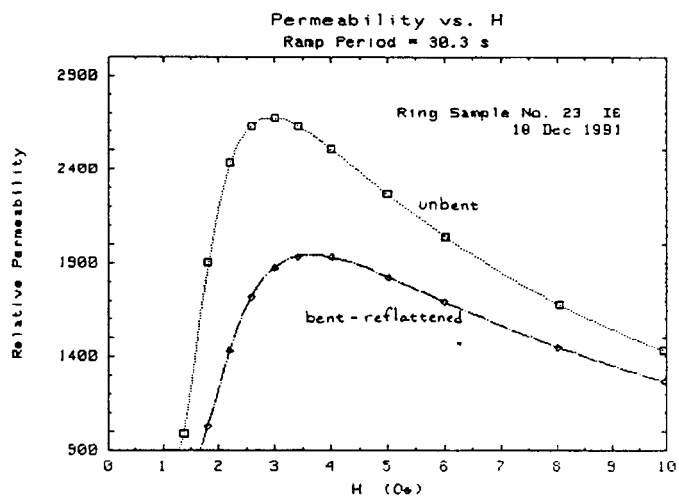

Figure 9. Comparison of the relative permeability, μ, of unbent and bent-reflattened steel samples.

Measurement Difficulties — Degaussing

The system was programmed to provide a single degauss before the first measurement was taken in both the H_c and the permeability runs. The measurements were always taken starting with the lowest H_{max} value. The original degaussing routine commanded the function generator to apply a 10 Hz sinusoidal waveform to the sample. The amplitude of the magnetizing field was set to 60 Oe and then reduced to zero in 100 steps with a step change occurring once every two cycles.

It was found that if the sample had first been subjected to a high field (e.g., 100 Oe), then the B values were lower for the first set of measurements (at values of H below the permeability peak) than for subsequent sets. The initial degaussing procedure was therefore inadequate. It was modified so that the initial amplitude was 100 Oe instead of 60 Oe, and the

frequency was decreased from 10 Hz to 5 Hz. The rate of the stepped reduction was maintained at once every two cycles. With the modified degaussing procedure, the results at low fields no longer differed significantly from run to run.

A comparison was made of using a single degauss and taking the data in order of increasing H_{max} as opposed to a single degauss and taking the data in order of decreasing H_{max}. For most H_{max} values, there was no significant difference, but in the region of the permeability maximum (3.0 Oe to 4.0 Oe for Ring Sample No. 17), the second method gave larger B values. The largest increase in B was 2.1% at 3.0 Oe. There was, however, no significant change in the values at either the low or high ends (in the regions 0.4 to 1.0 Oe and 6.0 to 100.0 Oe) for this sample.

V. Future Work

Although the effect on the magnetic properties of lowering the temperature was investigated for a single ring sample, it is necessary to determine whether there is an increase in the spread of the H_c values, which will require measuring a larger number of samples. Also, the collider operates at liquid helium temperatures rather than at liquid nitrogen temperatures. A cryostat has been constructed to perform the measurements in liquid helium. With an H winding made of superconducting wire, magnetizing fields of up to 2000 Oe or more will be possible.

Acknowledgments

The authors acknowledge the assistance of Arup Ghosh, George Ganetis, and Meyer Garber in assembling the appropriate equipment. They also thank the members of the RHIC Steel Specification Task Force for their comments and encouragement.

References

[1] S. Kahn, “Analysis of Armco Magnet Steel for SSC”, MDN 374-30 (SSC-MD-262), February 20, 1991.

[2] See, for example, H. Laeger, F. Beco, S. Comel, J. Hostettier, R. Lüthi and L. Vuffray, “Production of the Soft Magnetic Steel Laminations for the LEP Dipole Magnets”, IEEE Trans. on Magnetics, **24**, No. 2, March 1988.

[3] S. Kahn, “Mechanical Analysis of the Yoke for the RHIC Arc Dipole Magnet”, MDN 386-7 (RHIC-MD-115) July 23, 1991.